ESR Study of Heisenberg Spin Exchange in a Binary Liquid Solution near the Critical Point*

JOHN C. LANG, JR. AND JACK H. FREED
Department of Chemistry, Cornell University, Ithaca, New York 14850

(Received 26 July 1971)

A careful study of the Heisenberg spin-exchange contribution ω_{HE} to the ESR linewidths of the di-*t*-butyl nitroxide (DTBN) radical dissolved in mixtures of 2,2,4-trimethylpentane and *n*-perfluoroheptane was performed. The study includes samples of different radical concentration dissolved in the critical composition of the two solvents. This critical solvent system is known to exhibit an anomaly in the macroscopic kinematic viscosity ν near T_c. It is found that in the critical region, ω_{HE} is *not* linear in T/ν. However, it was observed that ω_{HE} is linear in T/ν' both for noncritical compositions and critical compositions above T_c. Here ν' is the macroscopically measured viscosity, but with the "anomalous portion" subtracted out. Deviations from ideal behavior of ω_{HE} with respect to T/ν were observed and discussed. The experiments near the critical region required temperature stability and control to within ± 0.01°C at the ESR sample, and a description is given of the experimental design.

I. INTRODUCTION

There is much current interest in transport coefficients in the region of critical points.[1–3] Theories of critical fluctuations have been extended to predict the magnitude of anomalies in the transport coefficients,[4,5] and one may hope to test these theories experimentally. Because several relaxation mechanisms in ESR are dependent on the transport coefficient ν, the kinematic viscosity, it was believed that any critical anomalies in this coefficient might be manifested in the spin relaxation observables. Recent measurement of ν by macroscopic techniques for a variety of binary liquid solutions[2,3,6] have encouraged the belief that there is generally a critical anomaly in ν. We chose to study one such binary liquid mixture (which is known to have a large critical anomaly in ν) by introducing into it small amounts of a well-characterized and stable organic free radical soluble in both components. The primary relaxation mechanism that we chose to focus on in our experiments is Heisenberg spin exchange, which depends on the translational diffusion rates of the radicals.[7] Thus, if the "microscopic viscosity" affecting radical motions corresponds to the macroscopic viscosity, an anomaly in the latter should manifest itself in the temperature dependence of this relaxation process.

Strong Heisenberg spin exchange is a diffusion-controlled relaxation process[8,9] where in the slow exchange limit (*viz.* the ESR hyperfine lines remain well resolved)

$$\omega_{HE}=\tau_2^{-1}=(\sqrt{3}/2)f_{\bar{m}}\,|\,\gamma_e\,|\,[\delta_{\bar{m}}-\delta_{\bar{m}}(0)]. \qquad (1)$$

In Eq. (1) ω_{HE} is the Heisenberg exchange frequency, and τ_2 is the mean time between successive new bimolecular encounters of radicals; $\delta_{\bar{m}}$ and $\delta_{\bar{m}}(0)$ are ESR linewidths of the line of spectral index $\bar{m}$ in the presence and absence of exchange, respectively. $f_{\bar{m}}$ is a simple statistical factor for each hyperfine line[8]; γ_e is the gyromagnetic ratio of the electron. τ_2 may be related to the radical diffusion coefficient D by

$$\tau_2^{-1}=4\pi dDf\mathfrak{N}, \qquad (2)$$

where d is the encounter distance of two radicals undergoing exchange, $\mathfrak{N}$ is the number density of radicals, and f is equal to unity for uncharged radicals. In the Stokes–Einstein limit we may write

$$D=kT/6\pi a\eta, \qquad (3)$$

where a is the molecular radius and η is the absolute viscosity equal to the product of ν and the density ρ. Equation (2) can be written in more useful form by letting $\mathfrak{N}=10^{-3}N_AC$ where N_A is Avogadro's number and C is the molar concentration; for on writing $C(T)=C_{T_0}[\rho(T)/\rho(T_0)]$ we may separate the temperature dependent from the temperature independent terms. Then Eqs. (1)–(3) lead to the following expression for the exchange contribution to the linewidth:

$$\delta_{\bar{m}}-\delta_{\bar{m}}(0)=A_{\bar{m}}^{-1}C_{T_0}[T/\nu(T)], \qquad (4)$$

where the temperature independent quantity $A_{\bar{m}}$ is defined as

$$A_{\bar{m}}=3\sqrt{3}\times 10^3 f_{\bar{m}}\,|\,\gamma_e\,|\,\rho(T_0)a/(4dfN_Ak). \qquad (5)$$

Thus Eq. (4) automatically includes the correction for concentration changes due to the temperature dependence of the density. In the event that there is a process, such as a chemical reaction at equilibrium, which causes a temperature-dependent change in the number of radicals, C_{T_0} becomes temperature dependent and is equal to the radical concentration in the solution at the temperature of interest multiplied by $\rho(T_0)/\rho(T)$. The dependence of the Heisenberg exchange linewidth on ν given by Eq. (4) is the basis for our experiments. Although recent ESR studies of Heisenberg exchange have been consistent with the Stokes–Einstein relation for the diffusion coefficient, we note from Eqs. (1) and (2) that the temperature dependence of $\delta_{\bar{m}}-\delta_{\bar{m}}(0)$ is more precisely a measure of the temperature dependence of ρD.

The well-investigated system of 2,2,4-trimethylpentane (*i*-octane) and *n*-perfluoroheptane, which is known to exhibit an anomalous macroscopic viscosity in the

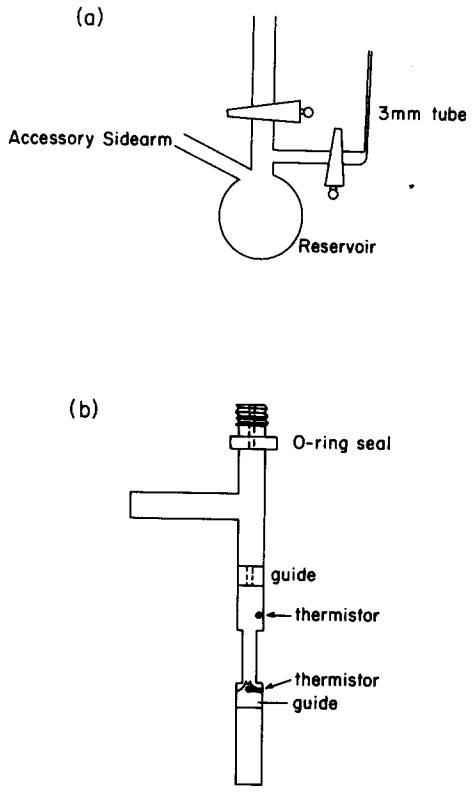

FIG. 1. (a) Diagram of the vacuum line sample assembly. (b) Diagram of the lucite sample holder and the bottom section of a phenolic O-ring seal cemented to it.

critical region,[10] was employed as the solvent in these experiments; di-*t*-butylnitroxide, whose Heisenberg exchange characteristics have been studied in a variety of other solvents,[8,9,11] was the stable organic free radical used. It is found to be soluble in all mixtures of the two solvents well beyond the range of temperatures and concentrations investigated here.

II. EXPERIMENTAL METHODS AND PROCEDURES

In order to investigate carefully the region of the critical point, it is necessary to prepare radical solutions by vacuum-line techniques in such a way that the solvent has a well-defined mole fraction composition of predetermined value. It is further necessary to have a temperature control which can maintain the ESR sample at a precise temperature to within 0.01°C near T_c. These experimental aspects are discussed below.

A. Materials

The perfluoroheptane was given to us by J. D. Lazerte of the 3-M Company. The iso-octane was spectranalyzed grade reagent obtained from the Fisher Scientific Company. Both chemicals were purified following the method of Hildebrand *et al.*[12] and were analyzed by gas chromatography using a F and M 700 chromatograph. The column found most effective in separating the *n*-perfluoroheptane from its isomers and other impurities had a liquid phase of hexadecane and a solid support of Chromosorb W. No impurity was detectable in the purified iso-octane by either gas chromatography or high resolution NMR. Eleven distinguishable compounds were observed in the unpurified perfluoroheptane. The normal isomer was in greatest abundance; it was identified by its infrared spectrum[13] and was concentrated on a Nester/Faust auto annular Teflon spinning band distillation column. Nonetheless, the fraction used in our experiments contained in addition to the normal isomer 28% of a second and 1% of a third isomer; they were identified as isomers on the basis of their boiling points, their infrared spectra,[13] their small effect on the value of the critical temperature of the solution with iso-octane, and the absence of hydrogen in any of the molecules (affirmed by mass spectroscopy). The critical temperature of our undoped binary solutions is 23.57°C and $\chi_{C_8H_{18}}$ of the critical mixture is 0.58; these compare well with the values of 23.65°C and 0.58, respectively, reported by Reed and Taylor. Since their C_7F_{16} was also known to contain approximately 10% of an isomer, the small difference in the two values of T_c was attributed to the difference in isomer content. The work of Bak and Goldburg[14] suggests such small differences in the constitution of the solvent should not alter the magnitude of the $T-T_c$ dependence of that portion of ν resulting from critical effects. The value of T_c is further shifted when the radical is added to the binary solution. Thus T_c increases to 23.79°C, 23.91°C, 24.31°C for respective radical concentrations of $1\times10^{-4}M$, $4.3\times10^{-3}M$, $6.2\times10^{-3}M$ in agreement with the observation that di-*t*-butylnitroxide is perferentially soluble in the hydrocarbon component.[15,16]

The di-*t*-butylnitroxide (DTBN) was synthesized by G. E. Samuelson following the method of Hoffmann and Henderson.[17] The purity of the radical, determined from the observed extinction coefficient, was increased to better than 95% by oxidation and vacuum spinning band distillation.

B. Sample Preparation

Because it was essential to maintain the purity of the prepared solvents as well as to prevent evaporation of these rather volatile components, all mixings and dilutions were accomplished by syringe injection of the components into reservoirs with serum bottle stoppers. The composition of the binary solvent was ascertained most accurately as a weight fraction. The approximate amount of radical was also determined by weight; its molar concentration was estimated from the density data of Reed and Taylor.

The design of the Pyrex sample assembly used for making all ESR samples is shown schematically in Fig.

1(a). Solutions of the radical dissolved in the pure components i-C_8H_{18} and C_7F_{16} were injected into this assembly through a serum bottle stopper in the accessory sidearm. After the last weighing, the accessory sidearm was removed in the usual fashion with the solution frozen in the reservoir. It was found that two high vacuum stopcocks were necessary for the assembly. The first, located between the vacuum line and the reservoir, was necessary to maintain isolation of the solution when the assembly was separated from the vacuum line during weighings and solution transfer into the sidearm (at $T>T_c$). The second stopcock was needed to prevent distillation of any component from the reservoir into the sidearm when the latter was placed in liquid nitrogen, sealed, and removed.

The assembly and the procedure outlined in the previous paragraph proved satisfactory for making ESR samples of reproducible composition in the binary solvents. This was easily verified by investigating the phase separation temperatures of two samples of nearly identical solvent compositions (by weight). Nevertheless, even though the standard precautions for vacuum line preparation of free radicals were followed, it was not possible to obtain reproducible concentrations of radicals. There were two likely reasons for this complication. The first is that DTBN is not very soluble in the C_7F_{16}, so it is possible that in the initial concentrated ($\sim 10^{-1}M$) solution not all the DTBN weighed out had dissolved. The second derives from the need for the volumes in the 3 mm o.d. sidearms to be small, and the fact that the O-ring stopcock when closed can capture a residual amount of solution that would distill over into the sidearm when the latter was frozen. It is suspected that only the volatile components distilled over into the sidearm and thus the less volatile DTBN was left on the walls of the stopcock; such a dilution would thereby alter the radical concentration from that calculated by weight. Therefore, it was found necessary to determine the radical concentration using standard ESR radical concentration measurements.

The 3 mm tubes finally used in the ESR study were about 2-in. long and were approximately $\frac{2}{3}$ filled with solution. Samples of such short lengths allowed the magnitude of the temperature gradient over the entire sample to be reduced to that of the temporal fluctuations.

C. Temperature Control

The temperature of the ESR sample was maintained by circulating Dow Corning 200 silicone oil from a constant temperature bath through the sample holder in the microwave cavity. Three aspects of this control will be described: (1) the design and characteristics of the constant temperature bath itself, (2) the manner in which the temperature was monitored in the bath as well as at the ESR sample, and (3) the design of the ESR sample holder.

The constant temperature bath is composed of a 7 gal capacity glass jar surrounded by Fiberglas insulation which is enclosed in an air-tight plywood box leaving access to the jar from the top. Circulation of the oil is provided by a Ruthman pump, Model TLO, which has a pumping capacity of 40 gal of water per min at a 10 ft head. The output of the pump is divided and throttled with a needle valve to control accurately the rate of flow outside the bath. The pump was modified to reduce thermal conduction between the motor and the bath by replacing the brass shaft with one of stainless steel and by embedding cooling coils in the brass stem housing. The oil being drawn into the pump passes through a cylindrical copper cooling tower and over a 500 W immersion heater wound to fit inside the cooling tower and to promote mixing. The tower is cooled at a precise rate by controlling, with a needle valve, the flow rate of a solution of antifreeze and water circulated from a Tamson bath, Model TEV-45. The source of cooling for the Tamson bath is a Neslab PBC-2 bath cooler. A resistor in series with the immersion heater is used to diminish the tendency for thermal oscillation. The oil leaving the pump passes either out of the bath to maintain the temperature of the ESR sample or directly back into the body of the bath flowing against the sensor of the Bayley temperature controller, Model 123. Random mixing in the oil is promoted by a small stirring motor. It reduced the magnitude of temperature fluctuations by a factor greater than 3. A top was fashioned of plywood lined with foam rubber to fit tightly about the structures protruding above the jar. The maximum excursion of the temperature in the constant temperature bath is ± 0.005°C over the period of an hour, when the heating rate and coolant flow are optimally set and no manual corrections are made.

Absolute temperature measurements were made utilizing the resistance of thermistors calibrated by the Yellow Springs Instrument Company against a platinum resistance thermometer which had been calibrated by the National Bureau of Standards. Their accuracy at the time of arrival was ± 0.01°C. The value of the resistance is measured by using an ac Wheatstone bridge which employs a 7 decade resistor in its third arm and a lock-in amplifier, designed similar to the Princeton Applied Research (PAR) JB-5, as the null detector. A PAR platinum resistance thermometer, Model PT-2, could be used to determine relative temperatures of the oil in the constant temperature bath, although its absolute calibration was found to be insufficiently accurate.

A diagram of the Lucite sample holder appears in Fig. 1(b). The choice of dimensions of the central portion inserted in the Varian V-4531 brass cavity was constrained by the conflicting requirements of unhindered flow and maximum cavity quality factor. The thermistors embedded in the lucite both above and

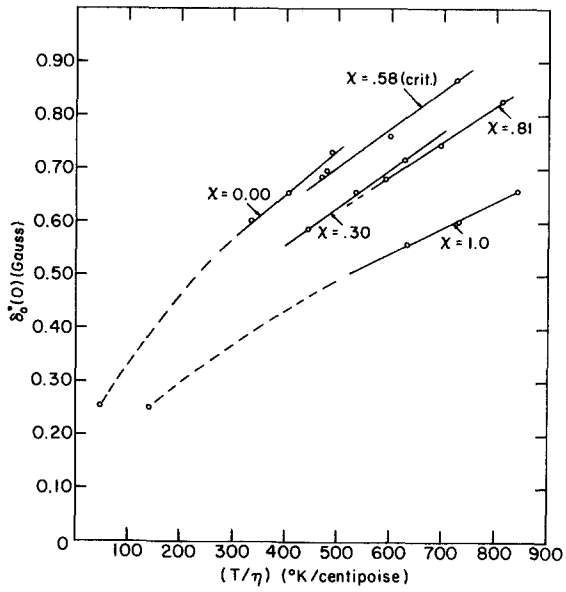

FIG. 2. $\delta_0^*(0)$ vs T/η for $1\times10^{-4}M$ DTBN in solutions of different solvent composition. χ is the mole fraction of i-C_8H_{18} in the solvent.

below this region where the sample is positioned allow determination of the absolute temperature at, the fluctuations near, and the gradient over the sample. The rate of flow past the ESR sample is regulated so that the fluctuations and gradient are minimized; because of joule heating effects, lower flow rates are used at temperatures near ambient. The maximum gradient observed over the samples could be maintained at the level of the long term fluctuations, ±0.01°C, for the entire temperature range investigated so long as the room temperature was kept below 69°F. Rapid access to the samples, necessary for providing thorough mixing at temperatures greater than T_c, is facilitated by placing the constant temperature bath so that the surface level of the oil is below the bifurcation level of the holder. The critical temperatures were determined by observing the samples in the polished central section of the lucite holder when it was located outside the microwave cavity.

D. Linewidth and Radical Concentration Measurements

All of the linewidth data collected for the solutions with the mixed solvents were obtained on a Varian V-4502-14 X-band ESR spectrometer described elsewhere[8] but modified by the inclusion of a V-4542 field/frequency lock driven by the same voltage as the x axis of the X–Y recorder and by the substitution of an improved lock-in detector. Other linewidth measurements were made with either the above assembly or a Varian E-12 spectrometer.[18] The magnetic field sweep was calibrated with a sample of potassium tetracyanoethylene dissolved in dimethoxyethane.[19a] With the ESR system in the configuration just described, the absolute linewidths were reproducible to within $\pm1\%$ from one day to another; in fact, the field/frequency lock provided a field of sufficient reproducibility that its calibration changed at most by $\pm1\%$ over a period of a few months. Two other precautions were followed: The microwave power was maintained at a uniform level at which no appreciable saturation occurred; the radical concentrations were chosen so that $\omega_{HE}<0.3a$ in order that Eqs. (1)–(5) for the slow exchange limit apply.[8,9]

Eastman *et al.*[8] showed how the stable radical DTBN could be used as a standard for determining the absolute spin concentrations from double integrations of the EPR first derivative signals. Since the purity of the DTBN had already been determined, the absolute concentration of the radical in a one-component solvent could be calculated from the weight of the two constituents. It was necessary to use a sample assembly of simpler design than that in Fig. 1(a) and so avoid introducing changes in radical concentration, and to follow the techniques described in Sec. II.B for handling volatile compounds. The assembly used for the standards was identical with that in Fig. 1(a) except there were no stopcocks. The reproducibility of these standards was demonstrated by the fact that they all gave spin concentrations in the ratios predicted by the weight concentrations. All spin concentration measurements were performed at a room temperature elevated above T_c.

III. EXPERIMENTAL RESULTS

The ESR linewidth of the central hyperfine line of di-t-butylnitroxide was examined as a function of temperature, composition of the solvent (given as the mole fraction, χ, of C_8H_{18}) and concentration of the radical. The temperature range investigated was from 45°C to either 21°C or the critical temperature, whichever was greater. The linewidths in the absence of appreciable exchange, $\delta_0(0)$, were determined from studies at $1\times10^{-4}M$ concentration. These linewidths include significant contributions from small unresolved t-butyl proton hyperfine structure,[9] and one must correct for this to obtain the correct intrinsic widths $\delta_0^*(0)$, in the absence of such structure. The details of this procedure are given in the Appendix. It should be noted that these solutions are of sufficient dilution that the spin-exchange contribution to $\delta_0^*(0)$ was less than 4%, as estimated from the studies at higher concentrations, and the small corrections for this are made as needed (see below). These linewidths $\delta_0^*(0)$ are shown as functions of T/η in Fig. 2. For each χ investigated, two solutions of higher concentration in radical were studied; all of these solutions between $10^{-2}M$ and $10^{-3}M$ in DTBN exhibited linewidth behavior interpretable on the basis of Eq. (4) as due to exchange broadening. The linewidths for these samples of higher radical concentration were also corrected for the contribution from un-

resolved proton structure, a contribution now greatly diminished by exchange narrowing of the envelope of the proton hyperfine components (see Appendix).

The temperature dependence of the exchange linewidth $\delta_0^*-\delta_0^*(0)\equiv W$ for the solutions of stated radical concentration and solvent mole fraction is displayed in Fig. 3. Each point on this plot represents the average of 3–8 measurements of the linewidth. Linewidths measured more than four times were generally obtained on different days, and the average value of all the measurements were used even though the scatter was never more than $\pm 1\%$. Several of the lines including all χ_c in Figs. 2, 3, and 4 were obtained from independent runs taken several weeks apart. It should be emphasized that the uncertainty in our measurements is, nonetheless, attributed entirely to the determination of the linewidths, since the temperature was monitored throughout every experiment and its stability of ± 0.01°C results in a negligible change in the linewidth (see Fig. 3). The solid lines in the figure are used to emphasize the data for solutions of critical composition. Before explaining how the curved lines in Fig. 3 were calculated, it is important to note for the noncritical solutions the excellent fit of the experimental data to straight lines of the form

$$W=E_0[T/\nu]+F_0 \qquad (6)$$

as shown in Fig. 4. The existence of nonzero intercepts in excess of the experimental error are not expected

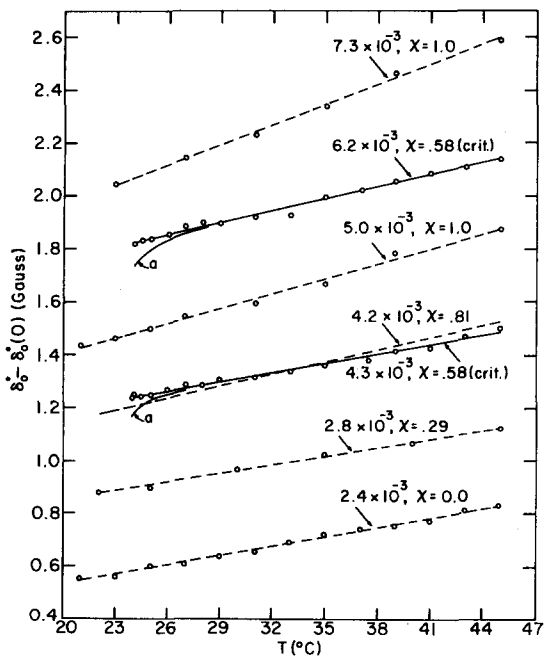

FIG. 3. Heisenberg spin exchange linewidth, corrected for proton hyperfine structure, for the $\bar{m}=0$ line of DTBN in solutions of indicated radical concentration and solvent mole fraction composition vs T. (See text for an explanation of curves marked "a".)

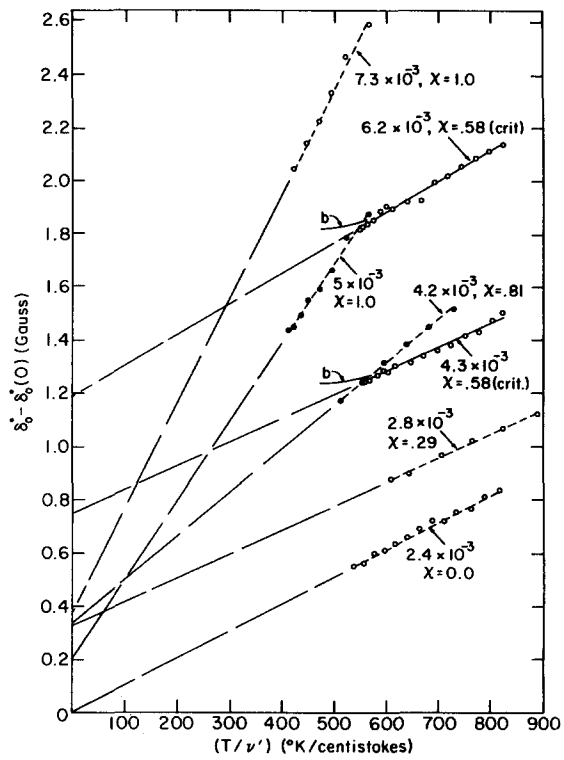

FIG. 4. Heisenberg spin exchange linewidth, corrected for proton hyperfine structure, for the $\bar{m}=0$ line of DTBN in solutions of indicated radical concentration and solvent mole fraction composition vs T/ν'. (See text for an explanation of curves marked "b".)

from Eq. (4) and will be dealt with in the next section. We first made the assumption that this linearity would be unaltered by the onset of critical phenomena. Therefore, in order to estimate the magnitude of the anomaly predicted in the temperature dependence of the linewidth, we determined the coefficients E_0 and F_0 for the critical solutions at temperatures outside the critical region ($T-T_c>7$°C) and then used these values in Eq. (6) to calculate W in the critical region from the macroscopic viscosities (as functions of $T-T_c$) previously reported.[10] The curved lines (marked "a") in Fig. 3 are plots of such hypothetical W's. [One compares the differences in $\delta_0^*-\delta_0^*(0)$ between the curves and the straight lines at constant temperature.] It is seen that the calculated curves "a" depart significantly from the experimental observations, and we infer from this that the viscosity regulating the rate of spin exchange is not the same viscosity ν observed by macroscopic methods. This same conclusion is illustrated in another way in Fig. 4. In this figure we introduce a new variable ν', which is defined to be identical to ν outside the critical region and equal to the linear extrapolation[19b] of ν from outside the critical region in the critical region. The linewidths of all samples of *noncritical* composition are observed to be linear in T/ν'

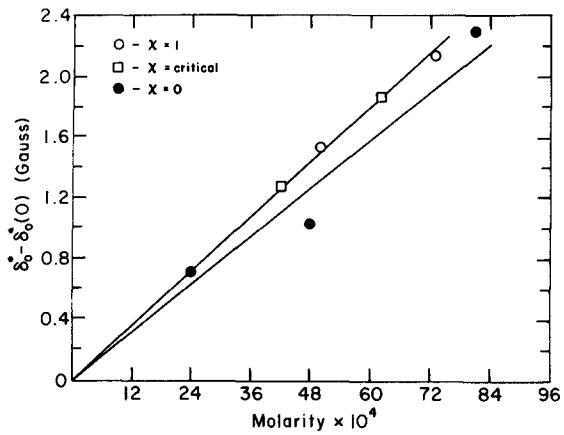

FIG. 5. Heisenberg spin exchange linewidth, corrected for proton hyperfine structure, for the $\bar{m}=0$ line of DTBN vs radical concentration at 27°C.

(which is the same as T/ν). The linewidths of samples of *critical* composition are also observed to be linear in T/ν' even in the critical region where T/ν' now is *not equal* to T/ν. The curves "b" are obtained when W is plotted as a function of T/ν; the straight lines result when W is plotted as a function of T/ν'. The discrepancy from a linear fit in T/ν is most easily seen by comparing T/ν and T/ν' at *constant* $\delta_0^*-\delta_0^*(0)$. (This reflects the fact that ν is significantly larger than ν' in the critical region.) Alternatively, if the observed linewidths were linear with T/ν in the critical region (as they are away from that region), then they would have fallen along the straight lines (instead of on curves "b") but along the portion extrapolated to the values of T/ν corresponding to those values in curves "b." Therefore both Fig. 3 and Fig. 4 show that the observed linewidth 0.01°C above the critical point is over 70 mG broader than predicted on the basis of a linear dependence of W on T/ν. In summary our results shown in Figs. 3 and 4 agree well with a linear dependence of W on T/ν' but not on T/ν.

A linear least squares analysis of the data in Fig. 4 was made. The lines drawn in Fig. 4 represent the linear least squares solutions. For the noncritical samples, E_0 and F_0 were computed from the linewidths as a function of T/ν, while for the critical samples E_0 and F_0 were computed from the linewidth as a function of T/ν'. The observed linewidth is linear in the concentration; this is exhibited in Fig. 5 for all values of χ investigated. We, therefore, present the "normalized" intercept F_0/C and slope E_0/C in Figs. 6(a) and 6(b), respectively, as functions of χ. The uncertainty in these values is governed by the accuracy of the radical concentration measurements and is believed to be $\lesssim 10\%$.

An estimate of the rate constant k at 30°C for the bimolecular exchange "reaction" was obtained from E_0/C [as though Eq. (4) were valid] and is plotted as a function of χ in Fig. 6(c). The theoretical rate constant was calculated for diffusion of a particle in the Stokes–Einstein limit.[8] Eastman *et al.*[8] also showed that k could be computed from the slope of W vs radical concentration. The value so determined from Fig. 5 for both the critical mixture and pure iso-octane was $6.3\times10^9 M^{-1}\cdot\text{sec}^{-1}$ (at 30°C). This result for pure iso-octane is in good agreement with the value of $6.0\times 10^9 M^{-1}\cdot\text{sec}^{-1}$ obtained from the T/ν dependence of W and shown in Fig. 6(c). [This value of k is also close to the absolute magnitude of $7.6\times10^9 M^{-1}\cdot\text{sec}^{-1}$ calculated from Eqs. (1)–(3).] However, for the solution of critical composition, this result of $6.3\times10^9 M^{-1}\cdot\text{sec}^{-1}$ obtained from the concentration dependence is in marked disagreement with the value of $2.8\times10^9 M^{-1}\cdot\text{sec}^{-1}$ calculated simply from the T/ν' dependence of W. Therefore, whereas the results for the pure solvent are consistent with our analysis in terms of strong exchange and the Stokes–Einstein relation, the results for the critical mixture display a notable deviation from the predictions of that analysis. The origin of this disparity will be discussed in the subsequent section; there it is shown the correct measure of exchange is provided by the concentration dependence of the linewidth. We may note, however, in anticipation of the discussion below, that if the exchange rate constant for the *mixture* is calculated from a plot of the observed exchange line-

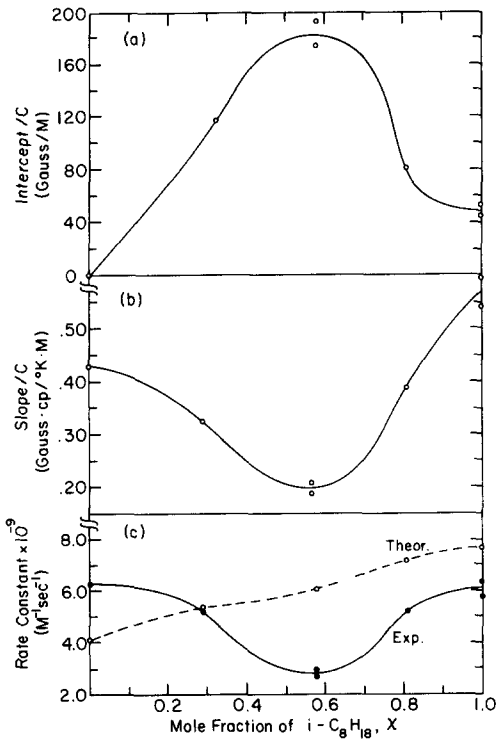

FIG. 6. E_0/C_{T_0} (a), F_0/C_{T_0} (b), and theoretical and experimental rate constants (c) vs χ. $k_{\text{exp}}=(E_0/C_{T_0})\ (T/\nu')_{T_0}$ 2.28×10^7 sec$^{-1}\cdot M^{-1}$.

widths vs the T/ν values corresponding to *pure isooctane*, then not only are the anomalously large intercepts decreased to a small fraction of their previous values but the rate constant calculated is $5.5\times10^{9}M^{-1}\cdot$ sec^{-1}, in better agreement with that obtained from the concentration dependence.

IV. DISCUSSION

A. Noncritical Region

The dependence of the Heisenberg spin exchange linewidth on viscosity was given by Eq. (4), yet some of our experimental results departed from this relation by the presence of nonvanishing intercepts. Before discussing the features of our results specific to any critical effect, it is important to examine how these intercepts might arise and to show they would not obscure the observation of an anticipated critical anomaly.

Whatever the source of the intercepts, they are observed to change with χ and must derive from an additional dependence on temperature. Yet the true linewidth remains linear in concentration. For these reasons we can describe the effect phenomenologically by letting the expression for the observed linewidth be of the form

$$W(T,\chi,C_{T_0})=A_0^{-1}C_{T_0}[T/\nu]g(T,\chi). \tag{7}$$

Since the experimental results illustrated in Fig. 4 are consistent with a linear dependence on T/ν over the range studied, then a simple Taylor series expansion of W in $T/\nu\equiv Z$, with only the linear term retained, can be used to correlate the data. Thus,

$$W_l(Z,T_0,\chi,C_{T_0})=W(T_0,\chi,C_{T_0})\times[ZZ_0^{-1}+g'(T_0,\chi)g^{-1}(T_0,\chi)(Z-Z_0)], \tag{7'}$$

where W_l is the linear approximation to W in the region about T_0, g' the derivative of g with respect to Z, and $Z_0\equiv T_0/\nu(T_0,\chi)$. [We have no reason for expecting $g(T,\chi)$ to be linear over a *wide* temperature range.] The intercept and slope of Eq. 7′ as a function of Z are, respectively,

$$F_0\equiv W_l(0,T_0,\chi,C_{T_0})=-Z_0W(T_0,\chi,C_{T_0})g'(T_0,\chi)g^{-1}(T_0,\chi), \tag{8a}$$

$$E_0=W(T_0,\chi,C_{T_0})[Z_0^{-1}+g'(T_0,\chi)g^{-1}(T_0,\chi)]. \tag{8b}$$

One is also interested in the slope of Eq. 7′ as a function of C_{T_0} at Z_0; this is simply

$$E_2=C_{T_0}^{-1}W(T_0,\chi,C_{T_0})=A_0^{-1}Z_0g(T_0,\chi). \tag{8c}$$

Thus the experimental observables $E_0(T_0,\chi,C_{T_0})$, $F_0(T_0,\chi,C_{T_0})$, and $E_2(T_0,\chi)$ are related by

$$E_0=[E_2C_{T_0}-F_0]Z_0^{-1}. \tag{8d}$$

Equations (8) can be used as a partial check on the consistency of our data. For example, E_0 calculated by a least squares analysis of the data presented in Fig. 4 for the solution in which $\chi=0.58$ and $C_{T_0}=4.3\times10^{-3}M$ is 8.88×10^{-4} G·cP·°K^{-1}; E_0 calculated from both Eq. (8d) and the E_2 presented in Fig. 5 for the solution in which $\chi=0.58$ (corrected to the value of T_0 equal to 30°C) is 9.8×10^{-4} G·cP·°K^{-1}. The difference in these two values could result from only a 4% error in the concentration measurement [cf. Eq. 8d)] and this is within the experimental uncertainty of that quantity. Inclusion of the much smaller intercepts for the samples of noncritical composition similarly promote greater agreement between E_0 calculated from E_2, and E_0 observed from the temperature dependence of the linewidth. Equations 8 can also be used to support our earlier assertion that the concentration dependence of the linewidth is the better parameter from which to determine the rate constant. For from Eq. (8c) it follows that

$$k=(\sqrt{3}/2)f_{\bar{m}}\,|\,\gamma_e\,|\,E_2.^{8} \tag{9}$$

An equivalent simple expression containing just E_0 cannot be written. Furthermore, from Eqs. (7), (8c), and (9) it is apparent that the presence of $g(T,\chi)$ not equal to unity is equivalent to asserting k deviates from the value predicted by the simple hydrodynamic model.

The function $g(T,\chi)$ can arise from a number of phenomena, and some possibilities will be reviewed in the remainder of this section. Since we have found W is a linear function in C_{T_0} (cf. Fig. 6), then g is not a function of C_{T_0}. This rules out the possibility that a process such as radical dimerization is the source of the additional temperature dependence in the linewidth; therefore such possibilities have been neglected in the subsequent discussion.

Previous work has shown that the probability of exchange on radical–radical encounter may be temperature dependent.[8,9] Such a dependence occurs in the limit of weak exchange when this probability is reduced from the strong exchange value of $\frac{1}{2}$. In these situations ω_{HE} takes on the more general form: the product of τ_2^{-1} and the probability of exchange per encounter. In this case g, in Eq. (7), becomes the probability for exchange[8]:

$$g=[1+(J\tau_1)^{-2}]^{-1}, \tag{10}$$

where $-J$ is twice the exchange integral and τ_1, the mean lifetime of an exchanging radical pair, is for a Stokes–Einstein model proportional to η/T. For a number of reasons, however, weak exchange is an unlikely source of the additional temperature dependence. If Freed's expression for τ_1 is assumed,[8] the value of $J\tau_1$ for DTBN in pentane given by Plachy and Kivelson[9] may be scaled to give $(J\tau_1)^2\cong24$ for the binary solvent of critical composition at 30°C. Such a large value implies strong exchange! This value of $(J\tau_1)^2$ is much larger than the values of 2.5 and 2.2 calculated from

the experimental intercepts for the two critical solutions in which the radical concentrations were 4.3×10^{-3} and $6.2\times10^{-3}M$, respectively. These latter values of $(J\tau_1)^2$ are therefore inconsistent with both our current results and those of Plachy and Kivelson for exchange in one-component solvents, and with each other since τ_1 should be independent of radical concentration.

Despite our arguments against the presence of weak exchange, we wish to show how weak exchange, if present, would affect our observation of a critical anomaly in the viscosity. If Eq. (10) is expanded, for $(J\tau_1)^{-2}<1$, to lowest order, then

$$g\cong[1-(J\tau_1)^{-2}]. \tag{11}$$

Since τ_1^{-1} is proportional to D, which decreases with decreasing temperature, g will increase with decreasing temperature. That is, the slope of W vs T/ν will increase on lowering the temperature; because $W_l(T, T_0, \chi, C_{T_0})$ is determined at $T_0>T_c$, $W[T_c]<W_l[T_c]$. However, even when the smaller values are used for $(J\tau_1)^2$, the change in τ_1 from 30° to T_c would cause an *increase* in the reduction of the linewidth on approaching T_c of approximately 10%. (Such a deviation would be diminished if the anomalous increase in viscosity were not manifested.) Therefore, we conclude that weak exchange, though probably not the source of the large intercepts, would not, in any event, obscure the observation of an anomalous increase in the viscosity.

It has been observed for mutual diffusion in mixed solvents, and so might be expected for self-diffusion, that ηD need not be merely a product of a constant and the temperature.[20–23] This is a consequence of the nonideality of the solution. If we let

$$\eta D\equiv Th(T, \chi),^{24,25} \tag{12}$$

then g can be given by

$$g=(6\pi a/k)h(T, \chi). \tag{13}$$

Eyring *et al.*[21] explained the form of Eq. (12) in terms of absolute reaction rate theory and showed that their calculated results concurred with experimental findings of Lemonde.[20] In another explanation, Anderson and Babb[22] showed deviations from ideality could result from the presence in their binary solutions of a third species, a one:one solvent A–solvent B complex. For our observable, W, a possible microscopic model yielding such a dependence could be a preferential random walk. We envision this random walk to result from the preferential solubility of the DTBN in the hydrocarbon component for which we have ample evidence. At each step there would be a somewhat greater probability of proceeding in the direction of the locally greater concentration of hydrocarbon. If the motions were, simplistically, broken down into two "orthogonal" paths, then the linewidth would be composed of two contributions, each with a probability proportional to the concentration of radical species moving along that "coordinate." Thus a simple expression for W is

$$W=[C_1/(C_1+C_2)]A_0^{-1}(T/\nu)C_1 +[C_2/(C_1+C_2)]A_0^{-1}(T/\nu)C_2. \tag{14}$$

If path 1 were understood to be the one in which radical diffusion preferred higher concentrations of hydrocarbon and path 2, higher concentrations of fluorocarbon, then for this simple model,

$$C_1=[1+y]C_{T_0}, \qquad C_2=[1-y]C_{T_0}, \tag{15}$$

so g becomes

$$g=[1+y^2], \tag{16}$$

where y is a measure of the preferential solubility. From free energy considerations g would be expected to decrease with increasing temperature, so g in Eq. (16) would produce positive intercepts in the linewidth as a function T/ν. A further refinement in our simple hypothetical model would be to replace ν on the right-hand side of Eq. (14) by ν_1 and ν_2 in the first and second terms, respectively, to account for differences in viscosity in the two "orthogonal" paths. This would tend to account for the observation from Figs. 5 and 6 that the slopes for χ critical were more characteristic of the radical in pure iso-octane than in the mixture.

Because of the paucity of data and the difficulty in discriminating between the different possibilities which could yield a $g(T, \chi)\neq1$, we are not at this time able to analyze the matter further. Nonetheless, from the linearity of W in T/ν for all solutions outside the critical region it is apparent that (unless g has an exactly cancelling critical effect) any anomaly should not be obscured.

In addition to Heisenberg spin exchange, there is another relaxation mechanism, spin rotation, which is dependent on the viscosity. The spin–rotational contribution to the linewidths can be estimated from the graphs of δ_0^* vs T/η given in Fig. 2 after the very small exchange contribution is subtracted from δ_0^*. We first do this in the manner of Plachy and Kivelson.[9] Using for the spin–rotational contribution to the linewidth[26,27]

$$T_2^{-1\,\mathrm{SR}}=(9\tau_R)^{-1}\sum_i(g_i-g_e)^2, \tag{17}$$

where τ_R is an isotropic rotational correlation time, one can readily obtain the expression for the hydrodynamic radius a of di-*t*-butylnitroxide:

$$a=[6.55\times10^{-8}k(\sum_i(\Delta g_i)^2)/12\pi M_0]^{1/3}, \tag{18}$$

where $\Delta g_i=g_i-2.0023$ and $i=x, y, z$, and M_0 is the slope of the concentration independent portion of the linewidth as a linear function of T/η. The value of the hydrodynamic radius calculated from our data is 1.4 Å. This agrees well with the result with *n*-pentane as

solvent of $a=1.8$ Å,[9] (which when corrected for more accurate g values[27] is 1.7 Å). The smaller value we obtain in solvents of larger molecular size probably indicates less damping of the radical reorientation due to larger "free volume." Any dependence of the radius on the solvent composition could not be resolved.[28]

There is an important criticism to this analysis, viz. the existence of nonzero intercepts for $\delta_0^*(0)$ of the order of 0.3 G. Plachy and Kivelson[9] did not carry out a complete analysis equivalent to that given in our Appendix for obtaining $\delta_0^*(0)$ from $\delta_0(0)$. Thus they could not resolve any such nonzero intercepts nor correct for the small effects of unresolved proton structure on the T/η dependence of these widths. It is not immediately clear from our experiments what the source of these intercepts is, although similar results have been previously reported.[27b] There is the possibility that effects of inertial motion and molecular reorientation (which begin to play an important role if the anisotropic intermolecular potential between radical and solvent molecules becomes weak) result in nonzero intercepts for our data obtained above room temperature.[26b,27b] Significant curvature of $\delta_0^*(0)$ would then be expected at much lower values of T/η.[27b]

B. Critical Region

The Heisenberg spin-exchange contribution to the ESR linewidths for the radical in one-component solvents showed the typical dependence on T/ν commonly seen and in agreement with the Stokes–Einstein relation, Eq. (3), for the radical self-diffusion coefficient. The spin-exchange contribution to the ESR linewidths for the radical in two-component solvents and even in solvents of critical composition outside the critical region showed the typical linear dependence on T/ν; but in these solvents nonzero intercepts, presumably due to mixing effects, became large. Yet Fig. 3 indicates there is no anomaly in the temperature dependence of ρD, measured by spin exchange, as the critical temperature is approached. For, if there were an anomaly, one would observe a deviation from linearity of the linewidth function at temperatures approaching T_c; the magnitude of the anomaly predicted on the basis of the Stokes–Einstein relation was included in Fig. 3 for both samples of critical composition to demonstrate that such an anomaly if present could be resolved. Since ρD shows no anomaly, the viscosity ν' related to D by the Stokes–Einstein relation can have no anomaly; however, since the macroscopic viscosity has been observed to have an anomalous increase, it is also apparent ν' is not precisely the true macroscopic viscosity. ν' is identified in Fig. 4, where, in order to obtain linearity of W with T/ν for temperatures near T_c, it was necessary to define a ν' which is the value of the viscosity extrapolated as a function of temperature from outside the critical region. Then $\nu'=\nu-\Delta\nu$, where $\Delta\nu$ is the contribution from critical effects. Such a separation has been suggested on the basis of the theoretical work of Fixman[4] and others[5]; what we have observed is that molecular diffusion is unaffected by $\Delta\nu$, the contribution shown[4,5] to be due to long-range correlation of concentration fluctuations with a characteristic length ξ.

Let us now comment on why Fixman's results as well as observations from light scattering indicate no anomaly might be expected in D obtained from Heisenberg spin exchange. The Stokes–Einstein formula relating the macroscopic viscosity to the self-diffusion coefficient is appropriate for an idealized model in the hydrodynamic limit; namely, where $|\mathbf{k}|\to 0$ or equivalently where $|\mathbf{k}| \ll |\mathbf{k}_{ch}|$ in which $\mathbf{k}$ is the wave vector of the probe and $|\mathbf{k}_{ch}|=2\pi/\lambda_{ch}$, where λ_{ch} is the characteristic length of the system. For normal liquids, $|\mathbf{k}_{ch}| \simeq 2\pi/$molecular diam, and for a radical diffusion probe $|\mathbf{k}| \lesssim |\mathbf{k}_{ch}|$; yet the deviation from hydrodynamic behavior is apparently small enough that usual results for spin exchange in normal liquids show reasonably good agreement with the Stokes–Einstein limit. However, when one investigates $\Delta\nu$, then $|\mathbf{k}_{ch}|=2\pi/\xi$. Since the length ξ reaches the order of 1000 Å near T_c,[29–31] $|\mathbf{k}| \gg |\mathbf{k}_{ch}|$ and the diffusion probe is too small to measure such a contribution to the macroscopic viscosity. In addition we may note that the correlation time of the critical fluctuations is of the order of 10^{-3} sec,[32] whereas ω_{HE} is of the order of 10^{-8} sec. That is, the fluctuations are static on the time scale of exchange.

Our results then suggest that there is no anomaly in either the component of the viscosity for which $|\mathbf{k}| \lesssim |\mathbf{k}_{ch}|$ or the radical self-diffusion coefficient. Our experiments, in agreement with the work of Allen *et al.* on tracer diffusion[33] and other investigations of self-diffusion measured by NMR,[1,34] suggest that the intermolecular potentials determining the friction coefficients for small molecules do not have singularities associated with the onset of critical phenomena.

ACKNOWLEDGMENTS

We wish to acknowledge helpful and stimulating discussions with Professor W. I. Goldburg and Professor B. Widom, and to thank Mr. G. V. Bruno for his help with the computer programs.

APPENDIX: CORRECTIONS FOR UNRESOLVED PROTON HYPERFINE STRUCTURE

Each of the three distinct ESR absorption lines of DTBN is an envelope of unresolved proton hyperfine lines.[9,35] It is thus necessary to resolve the "intrinsic" linewidth δ^* from that of the envelope linewidth δ, which is measured experimentally, since Eq. (1) is strictly correct for the intrinsic linewidths. The proton hyperfine splittings were first determined, as already discussed, by Weil and co-workers,[35] by obtaining spec-

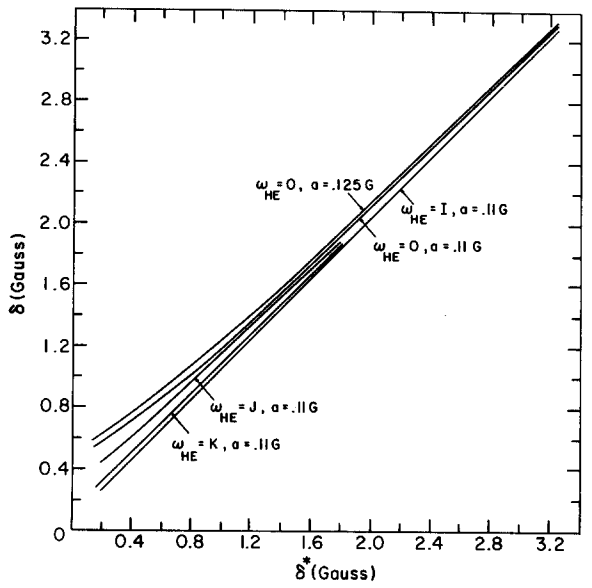

FIG. 7. Observed linewidth, δ, vs the intrinsic linewidth, δ^*, in the absence of any proton hyperfine contribution at different exchange frequencies and with different hyperfine splitting constants. $J=0.786\times10^7$ sec^{-1}, $K=2.25\times10^7$ sec^{-1}, $I=5.50\times10^7$ sec^{-1}.

tra of DTBN in pure solvents at low enough temperatures that the lineshape of each envelope shows a significant deviation from Lorentzian shape. (It was impossible to observe any proton structure even near the freezing points of the solvents.) By means of computer simulations, values of the proton hyperfine constant a_H, and the intrinsic derivative peak-to-peak Lorentzian width δ^*, could be accurately determined. We found $a_H=0.110\pm0.005$ G for $\chi=1$ and $a_H=0.125\pm0.005$ G for $\chi=0$ which are very close to the values found in other solvents. Given (1) the small differences between these two values of a_H and (2) the fact that studies in mixed solvents (which separate at low temperatures) could not be made at sufficiently low temperatures to get very significant deviations from Lorentzian lineshapes, we used the linear interpolation $a_H(\chi)=[0.125-0.015\chi]$ G.

The effects of an intrinsic linewidth $T_2(0)^{-1}\propto\delta^*(0)$, and of appreciable spin exchange ω_{HE}, respectively, tend to mask and to exchange narrow the unresolved proton structure. The analysis of these effects is straightforward.[36,37] Thus we may write coupled equations for each hyperfine component specified by N and M, the nitrogen and proton spin quantum numbers, respectively. They are written as $Z_{N,M}$ where $\mathrm{Im}Z_{N,M}$ and $\mathrm{Re}Z_{N,M}$ are proportional to the absorption and dispersion, respectively. Thus:

$$[\Delta\omega_{N,M}-i[T_2(0)^{-1}+\tfrac{2}{3}\omega_{HE}]]Z_{N,M}$$
$$-i\tfrac{1}{3}\omega_{HE}\sum_{M\neq M'}P_{M'}(Z_{N,M}-Z_{N,M'})=D_MA. \quad \text{(A1)}$$

Here $P_{M'}=D_{M'}/\sum_M D_M$ is the normalized statistical

TABLE I. Summary of the least squares slopes and intercepts for the corrected and uncorrected exchange linewidths as functions of both T and T/ν'.

χ (mole fraction)	C_{T_0} (molarity)	$E_0'\times10^3$ [a] gauss·cp °K^{-1}	$E_0\times10^3$ [b] gauss·cp °K^{-1}	F_0' [a] (gauss)	F_0 [b] (gauss)	$E_1'\times10^2$ [c] (gauss °C^{-1})	$E_1\times10^2$ [d] (gauss °C^{-1})	F_1' [c] (gauss)	F_1 [d] (gauss)
0	2.4×10^{-3}	0.921±0.023	1.03±0.03	−0.072±0.015	−0.002±0.022	1.07±0.03	1.20±0.03	0.189±0.009	0.290±0.011
0.29	2.8×10^{-3}	0.944±0.049	0.902±0.036	0.131±0.036	0.327±0.027	1.12±0.06	1.08±0.04	0.456±0.020	0.639±0.015
0.58 (crit)	4.3×10^{-3}	1.01±0.02	0.888±0.028	0.515±0.016	0.749±0.018	1.33±0.03	1.17±0.04	0.753±0.010	0.959±0.012
0.58 (crit)	6.2×10^{-3}	1.22±0.04	1.16±0.04	0.965±0.026	1.19±0.03	1.63±0.05	1.52±0.06	1.24±0.02	1.46±0.02
0.81	4.2×10^{-3}	1.70±0.07	1.63±0.07	0.137±0.044	0.339±0.041	1.59±0.07	1.53±0.06	0.656±0.022	0.839±0.021
1.0	5.0×10^{-3}	3.11±0.11	2.98±0.13	−0.058±0.051	0.202±0.060	1.95±0.07	1.87±0.08	0.807±0.024	1.03±0.03
1.0	7.3×10^{-3}	4.04±0.16	3.95±0.16	0.117±0.079	0.377±0.080	2.57±0.10	2.52±0.09	1.22±0.03	1.46±0.03

[a] From the linear least squares fits of the uncorrected linewidths to the form: $[\delta_0-\delta_0(0)]=E_0'(T/\nu)+F_0'$.

[b] From the linear least squares fits of the linewidth to the form: $[\delta_0^*-\delta_0^*(0)]=E_0(T/\nu)+F_0$, where the asterisks imply widths corrected for unresolved proton hyperfine structure.

[c] These are the linear least squares fits of the uncorrected linewidths to the form: $[\delta_0-\delta_0(0)]=E_1'T+F_1'$.

[d] These are the linear least squares fits of the linewidth to the form: $[\delta_0^*-\delta_0^*(0)]=E_1T+F_1$, where the asterisks imply widths corrected for unresolved proton hyperfine structure.

weight of the M'th proton hyperfine line and $D_{M'}$ is its degeneracy. Also $\Delta\omega_{N,M}=\omega-\omega_{N,M}$ with $\omega_{N,M}$ the Larmor frequency of the N, Mth line. The constant A is linear in our microwave field strength in the absence of saturation. Equation (A1) is valid only for the case of three well separated nitrogen lines (or $\omega_{HE}<0.3a$),[9] since we have neglected off-diagonal exchange terms between $Z_{N,M}$ and $Z_{N',M'}$ for $N'\neq N$.

Computer solutions of Eq. (A1) were obtained for an appropriate range of values of $(\sqrt{3}/2)\delta^*/|\gamma_e|\equiv T_2^{*-1}=[T_2(0)^{-1}+\frac{2}{3}\omega_{HE}]$ and ω_{HE}. We show in Fig. 7 the observed derivative linewidth of a nitrogen line, δ, as a function of δ^* for a range of values of ω_{HE}. The low-concentration intrinsic widths $\delta_0^*(0)$ for our experiments were easily obtained from the experimentally measured $\delta_0(0)$ and the curves in Fig. 7 for $\omega_{HE}\approx 0$. The higher concentration widths δ_0^* for our experiments were obtained by first estimating ω_{HE} from the uncorrected value of $\delta_0-\delta_0(0)$, so that the appropriate curve in Fig. 7 could be used. This then yields an approximation to δ_0^* from which a better value of ω_{HE} may be estimated. It was not necessary to repeat the iterative process suggested, since for the more concentrated solutions the convergence is so rapid. Note that though the curves are given for a specific value of a_H, they are readily scaled to other values of a_H. We also note that for the solutions with appreciable exchange, the residual width from the exchange narrowed proton structure may be approximated by the expression

$$(T_2)_{\text{residual}}^{-1}=(\gamma_e a_H)^2\sum_M P_M M^2[\tau T_2^*/(T_2^*+\tau)], \tag{A2}$$

where for DTBN $\tau^{-1}=\frac{1}{3}\omega_{HE}$ and $\sum_M P_M M^2=4.50$. This equation is adapted from a result given by Johnson[38] from a model[39] one may readily show to be applicable to Heisenberg exchange. Equation (A2) gave results in agreement within 1–2.5% with the curves shown in Fig. 7 for high exchange frequencies. The larger disagreement results for small values of δ^*.

The experimental results from linear least squares analyses of the linewidth are given in Table I. There we compare the results for the slopes (E) and intercepts (F) computed from both the uncorrected (primed) and corrected (unprimed) exchange widths as functions of T/ν' (subscript 0) and T (subscripted 1). We note only small differences as expected.

* Supported in part by the Advanced Research Projects Agency and by a grant from the National Science Foundation (Grant No. GP-13780).

[1] M. S. Green and J. V. Sengers (Eds.) Natl. Bur. Std. Misc. Publ. **273**, (1966).

[2] J. V. Sengers, "Transport Properties of Fluids Near Critical Points," University of Maryland, College Park, Tech. Rept. No. 71-074, 1970.

[3] G. Arcovito, C. Faloci, M. Roberti, and L. Mistura, Phys. Rev. Letters **22**, 1040 (1969).

[4] M. Fixman, Advan. Chem. Phys. **6**, 175 (1963).

[5] (a) K. Kawasaki, Phys. Rev. **150**, 291 (1966); (b) K. Kawasaki, Ann. Phys. **61**, 1 (1970).

[6] D. Woerman and W. Sarholz, Ber. Bunsenges. Physik. Chem. **69**, 319 (1965).

[7] G. E. Pake and T. R. Tuttle, Jr., Phys. Rev. Letters **3**, 423 (1959).

[8] M. P. Eastman, R. G. Kooser, M. R. Das, and J. H. Freed, J. Chem. Phys. **51**, 2690 (1969).

[9] W. Plachy and D. Kivelson, J. Chem. Phys. **47**, 3312 (1967).

[10] T. M. Reed III and T. E. Talyor, J. Phys. Chem. **63**, 58 (1959).

[11] M. P. Eastman, G. V. Bruno, and J. H. Freed, J. Chem. Phys. **52**, 2511 (1970).

[12] J. H. Hildebrand, B. B. Fisher, and H. A. Benesi, J. Am. Chem. Soc. **72**, 4348 (1950).

[13] *Fluorine Chemistry*, edited by J. Simons (Academic, New York, 1950), Vol. II.

[14] C. S. Bak and W. I. Goldburg, Phys. Rev. Letters **23**, 1218 (1969).

[15] I. Prigogine, *Treatise on Thermodynamics* (Longmans, Green, New York, 1954), Chap. 16. Prigogine shows that if a third component is much less soluble in one of the two major components than the other, T_c will be increased.

[16] The low concentration T_c is a bit higher than expected; we believe this may be due to a slight trace of moisture.

[17] A. K. Hoffmann and A. T. Henderson, J. Am. Chem. Soc. **83**, 4671 (1961).

[18] The E-12 spectrometer was obtained with the support of NSF Grant No. GP-10595.

[19] (a) S. B. Wagner, M. S. thesis, Cornell University, Ithaca, N.Y., 1970; (b) The data of Reed and Taylor for solutions of all values of χ show the viscosity to be linear in temperature over the restricted ranges investigated here in the absence of any viscosity anomaly. In viscosity studies on the pure solvents over extended temperature ranges the usual exponential dependence on temperature is observed [J. H. Simons and W. H. Wilson, J. Chem. Phys. **23**, 613 (1955); J. M. Geist and M. R. Cannon, Ind. Eng. Chem. Anal. Ed. **18**, 611 (1946)].

[20] H. Lemonde, Ann. Phys. **9**, 539 (1938).

[21] W. E. Roseveare, R. E. Powell, and H. Eyring, J. Appl. Phys. **12**, 669 (1941).

[22] D. K. Anderson and A. L. Babb, J. Phys. Chem. **65**, 1281 (1961).

[23] F. Dolezalek and A. Schulze, Z. Physik. Chem. **83**, 45 (1913).

[24] It can easily be shown from thermodynamic and hydrodynamic considerations [see L. D. Landau and E. M. Lifshitz, *Fluid Mechanics*, (Addison-Wesley, Reading, Mass., 1959), Chap. 6] that

$$D_1=D_2(\alpha_1/\alpha_2)(\partial \ln c_1/\partial \ln a_2)_{T,P}(\partial c_2/\partial c_1)_{T,P},$$

where D_1 is the self-diffusion coefficient of the radical and D_2 is the mutual diffusion coefficient of one of the binary solvent components. What we attempt to show in the remainder of Sec. IVA is that $h(T,\chi)$ could be dominated by either the first or the third term on the right-hand side of the above equation. We do not have enough data to distinguish the separate contributions. Anderson and Gerritz (Ref. 34) in a discussion of self-diffusion of one of the solvent components point out that both D_2 and their equivalent of $(\partial \ln c_1/\partial \ln a_2)^{-1}$ vanish at T_c, and suggest their divergences cancel so that D_1 need not have an anomaly at T_c. We believe it would be highly fortuitous to expect a precise cancellation. In fact, when the Stokes–Einstein limit applies (i.e., large particles), then $D_1\propto T/\nu$ and the weak but very definite critical anomaly in the macroscopic ν should manifest itself in D_1. In Sec. IV.B we suggest reasons for the breakdown of the Stokes–Einstein relation; the main point is not that there are singularities which cancel, but that the wavenumber dependence of D_1, D_2, and ν cannot be neglected.

[25] The similar nonzero intercepts observed in K^+TCNE^-–THF system (Ref. 8) might also be explained in such a manner. For this system the intercepts are smaller: only about 20% of the total width. It was originally suggested in Ref. 8 that the nonzero intercept was due to an additional lifetime broadening by the "chemical" process yielding an added width BC. An additional possibility exists in which a $g(T,\chi,C_{T_0})$ may be defined and interpreted in terms of an equilibrium constant $K(T,\chi)$ for the chemical process [J. C. Lang, Jr. and J. H. Freed (unpublished)].

[26] (a) P. W. Atkins and D. Kivelson, J. Chem. Phys. **44**, 169 (1966); (b) R. E. D. McClung and D. Kivelson, J. Chem. Phys. **49**, 3380 (1968).

[27] (a) J. S. Hyde, J. C. W. Chien, and J. H. Freed, J. Chem. Phys. **48**, 4211 (1968); (b) R. G. Kooser, W. V. Volland, and J. H. Freed, J. Chem. Phys. **50**, 5243 (1969).
[28] No critical anomaly was detected in the spin rotation portion of the linewidth; that is the "viscosity" determining angular momentum correlation had no observable contribution from critical effects.
[29] G. W. Brady, J. Chem. Phys. **32**, 45 (1960).
[30] B. Chu, Ann. Rev. Phys. Chem. **21**, 145 (1970).
[31] We may note that the average distance traversed between radical–radical encounters, as given by the Brownian motion expression $\langle(\mathbf{r}-\mathbf{r}_0)^2\rangle^{1/2}=(3/2\pi d\eta)^{1/2}$ is only of the order of 100 Å for $5\times10^{-3}M$ radical concentrations.
[32] P. N. Pusey and W. I. Goldburg, Phys. Rev. A **2**, 766 (1971).
[33] H. M. Leister, J. C. Allegra, and G. F. Allen, J. Chem. Phys. **51**, 3701 (1969).
[34] J. E. Anderson and W. H. Gerritz, J. Chem. Phys. **53**, 2584 (1970).
[35] R. J. Faber, F. W. Markley, and J. A. Weil, J. Chem. Phys. **46**, 1652 (1967).
[36] J. H. Freed, J. Chem. Phys. **45**, 3452 (1966).
[37] J. H. Freed, J. Phys. Chem. **71**, 38 (1967).
[38] C. S. Johnson, Jr., in *Advances in Magnetic Resonance*, edited by J. S. Waugh (Academic, New York, 1965), Vol. 1, p. 33, Eq. 12.
[39] H. S. Gutowsky, D. M. McCall, and C. P. Slichter, J. Chem. Phys. **21**, 279 (1953).

THE JOURNAL OF CHEMICAL PHYSICS VOLUME 56, NUMBER 8 15 APRIL 1972

Viscosity of Carbon Dioxide in the Temperature Range 25–700°C*

J. KESTIN, S. T. RO, AND W. A. WAKEHAM†
Division of Engineering, Brown University, Providence, Rhode Island 02912
(Received 19 July 1971)

The paper presents new relative measurements of the viscosity of carbon dioxide at a pressure $P=1$ atm and in the temperature range 25–700°C. The accuracy of the reported viscosity data is estimated as $\pm0.1\%$ at 25°C and $\pm0.3\%$ at 700°C. The rotational collision number for carbon dioxide is computed with the aid of the kinetic theory for polyatomic gases and reliable thermal conductivity data.

INTRODUCTION

The paper presents new relative measurements of the viscosity of carbon dioxide at a pressure $P=1$ atm and in the temperature range 25–700°C. The results constitute the first precise determination of the viscosity at the higher temperatures.

The kinetic theory of polyatomic gases, together with reliable data for the thermal conductivity, allows us to compute rotational collision numbers for carbon dioxide which are in substantial agreement with those obtained by direct measurement.

The experimental technique and the general arrangement of the instrument were the same as in Ref. 1. We assume that the reader is familiar with the earlier paper, and confine ourselves here to a presentation of the experimental results.

I. LIST OF SYMBOLS

A^*	Ratio of collision integrals
b	Spacing between the disk and the fixed plates
c_v	Specific heat at constant volume
$c_{\rm int}$	Contribution of the internal degrees of freedom to the specific heat
$c_{\rm rot}$	Contribution of the rotational degrees of freedom to the specific heat
$c_{\rm vib}$	Contribution of the vibrational degrees of freedom to the specific heat
d	Thickness of the disk
D	Total separation between the fixed plates
$\mathfrak{D}_{11}$	Self-diffusion coefficient
$\mathfrak{D}_{\rm int}$	Diffusion coefficient for internal energy
$\mathfrak{D}_{\rm rot}$	Diffusion coefficient for rotational energy
$\mathfrak{D}_{\rm vib}$	Diffusion coefficient for vibrational energy
$\mathcal{E}$	Einstein function
$f(T^*)$	Eucken factor for a polyatomic gas, Eq. (6)
$f_\mu^{(3)}$	Third order correction factor for the viscosity
$g(\zeta_{\rm rot})$	A function of the rotational collision number, Eq. (10)
H	A function of the internal specific heat and the rotational collision number, Eq. (12)
I	Moment of inertia of the suspension system
$\mathbf{k}$	Boltzmann's constant
k	Thermal conductivity
M	Molar mass
R	Radius of the disk
$\mathbf{R}$	Universal gas constant
T	Absolute temperature
T^*	Reduced temperature
T_0	Period of oscillation *in vacuo*
γ	A parameter of the (11–6–8) potential
δ	Boundary-layer thickness
Δ_0	Logarithmic decrement *in vacuo*
ϵ	Scaling factor for energy
ζ	Collision number
$\zeta_{\rm rot}$	Rotational collision number
$\zeta_{\rm vib}$	Vibrational collision number
Θ_i	Characteristic temperature of the ith vibrational mode of a molecule
μ	Viscosity
ρ	Density
σ	Length scaling factor
$\Omega^{(2,2)*}$	First order collision integral
Ω_{22}	Empirical collision integral